

CHROM. 10,698

## CHARACTERIZATION OF THE PHOTODIODE ARRAY DETECTOR IN LIQUID CHROMATOGRAPHY

MICHAEL J. MILANO\*, STANLEY LAM, M. SAVONIS, DAVID B. PAUTLER, JOSEPH W. PAV and ELI GRUSHKA

*Department of Chemistry, State University of New York at Buffalo, Buffalo, N.Y. 14214 (U.S.A.)*

---

### SUMMARY

In order to assess the viability of the photodiode array detector, its noise characteristics and linear range have been studied. It was found that at worst the peak noise is  $\pm 0.001$  a.u. but more typical values are  $\pm 6 \cdot 10^{-4}$  a.u. With increased signal averaging, the noise values can be decreased to  $\pm 2 \cdot 10^{-4}$  a.u. The detector was found to have a linear range between  $2 \cdot 10^3$  and  $6.5 \cdot 10^3$ , depending on the wavelength. The versatility of the diode array detector was demonstrated by deconvoluting a multi-solute chromatographic peak and determining the amounts of each solute in the mixture. The agreement between the amounts injected and those calculated was within several percent.

---

### INTRODUCTION

One of the most commonly used detectors in liquid chromatography is a UV spectrophotometer. Most often the detector is limited to fixed wavelengths, usually 254 nm or 280 nm, or both. The demand for a more versatile UV monitor for compounds that absorb in other regions of the UV spectrum has been met by instruments that can be set at a desired wavelength for any given run. More sophisticated commercial variable-wavelength detectors, by using stop-flow techniques, can scan and produce spectra of the solutes, but such procedures are time consuming. An alternative is to use rapid-scanning spectrometers, which include oscillating-mirror rapid-scanning instruments<sup>1</sup>, vidicon detectors<sup>2,3</sup> and solid-state photodiode array detectors<sup>4-10</sup>. All of these devices give multi-wavelength detection, yield the spectra of the components eluting in the same chromatographic run and allow the spectra to be stored for later analysis. Recently, a similar approach was used by Jadamec *et al.*<sup>11</sup> with a fluorescent detector.

The attractive features of the photodiode array have been discussed by Snow<sup>12</sup>, Dessy and co-workers<sup>6,7</sup> and Milano and co-workers<sup>9,10</sup>. The sensitivity of the photodiode array detectors can equal that of the fixed-wavelength detectors. The availability of a spectrum for each of the solutes in the mixture can be used for

---

\* To whom correspondence should be addressed.

identification, and deconvolution of overlapping peaks using first-derivative spectra has also been proved possible. Other advantages are improvement in quantitation, as the chromatogram can be displayed at the optimal wavelength for each solute, and enhanced detectability by summing the outputs of the elements in the photodiode array. The 5–500-fold increase in sensitivity can be useful in trace analysis<sup>8</sup>.

A detector, in order to be useful, should be sensitive, and its output should be linearly related to the amounts of solute sensed. To assess the sensitivity of the detector, its noise characteristics must be studied, as the noise determines the limits of detectability. This paper describes the noise characteristics of a photodiode array detector and the linearity of the device. In addition, several methods of deconvolution that permit the quantitation of several solutes under a single envelope are discussed.

## EXPERIMENTAL

### *Chromatographic conditions*

In the linearity study, a Tracor (Austin, Texas, U.S.A.) Model 500 pneumatic amplifying pump was used for solvent delivery. A Milton Roy (Laboratory Data Control, Riviera Beach, Fla., U.S.A.) duplex minipump was used in the studies of the detector noise characteristics and the deconvolution procedures. The columns used (either 250 × 4.1 mm I.D. or 250 × 2.1 mm I.D.) were slurry packed with Partisil 10 (Whatman, Clifton, N.J., U.S.A.). Injections were made with a 10- $\mu$ l high-pressure syringe (Precision Sampling, Baton Rouge, La., U.S.A.). The injector head was fabricated from Swagelok Union-T and PTFE-lined septum.

The detector cell was an 8- $\mu$ l LDC flow cell. The reference cell was not used.

### *Spectrometer system*

The deuterium lamp light source was powered by a Schoeffel (Westwood, N.J., U.S.A.) LPS 301 power supply, operated at 30 W and connected to a Sola (Elk Grove, Ill., U.S.A.) constant line voltage transformer. The polychromator, of a Czerny–Turner design, with a focal length of 150 mm, and a 1200 lines/mm grating blazed for 240 nm (Edmund, Barrington, N.J., U.S.A.) was built in-house. A 73-nm range (227–300 nm) was imaged over the 13-mm active area of the photodiode array. An entrance slit width of 0.5 mm was used, giving an overall resolution of approximately 3 nm.

A single Reticon (Sunnyvale, Calif., U.S.A.) 256-element photodiode array (RL256EC/17) was used as the detection element. The control circuits (RC200/204) and signal-processing circuits (CASH-1B-1) were also obtained from Reticon and used without modification.

The spectrometer was interfaced to a Data General (Southboro, Mass., U.S.A.) Nova II computer with a 16K core memory and two Data General floppy disk drives (Model 6030). Data were acquired and displayed through a high-speed (100 kHz) interface with a 12-bit, 8-channel analog-to-digital converter and two 12-bit digital-to-analog converters (ADAC Model 500-DCG-8-DI-APG-A-DMA). All programs were written in BASIC with assembly language subroutines for data acquisition and display.

The control circuits of the diode array were adjusted to produce a spectrum every 2.6 msec with an 11.7-sec delay between each spectrum, during which the

spectra were added to a running sum buffer. Although the diode array contains 256 elements, only 128 elements from alternate diodes are stored. Each spectrum that was recorded on the floppy disk and displayed on a CRT was the average of either 20 or 94 spectra. Averaging 20 spectra required 1 sec while averaging 94 spectra took 2 sec. A total of 250 spectra were recorded for each experiment.

### *Procedure*

Prior to each experiment, a spectrum was recorded with the light beam blocked and subtracted from all other spectra to account for the finite dark current of the diodes. A reference spectrum of the mobile phase was also recorded at the beginning of each experiment and was used in the calculation of absorbance for the data spectrum. The solutes were then injected. When the retention times were long, data collection began at 150 sec after the injection. The chromatogram can be displayed at any single wavelength in real time on a storage oscilloscope. After completion of the experiment, numerous data processing programs were used to evaluate the data.

During the linearity study the flow-rate was 0.45 ml/min while during the deconvolution it was 0.58 ml/min. These two studies were carried out on two different columns.

The data for the linearity study were collected in 1 day. The various concentration solutions were prepared from a stock solution.

### *Reagents*

The mobile phase was spectro-analysed *n*-heptane. The solutes used were of either reagent grade or spectral grade.

## RESULTS AND DISCUSSION

### *System noise*

There are several sources of noise in the rapid-scanning spectrometer, including fixed pattern and random noise in the detector, lamp drift and sampling errors. The fixed pattern noise can be as much as a few percent of the voltage output of the Reticon array and is due to a combination of switching glitches, dark current and sensitivity variations among the diodes. To reduce the effect of the switching glitches, a 50-kHz, three-pole, active filter was used at the output of the signal processing, CASH-1B-1, circuits. In addition, the A/D converter on the computer interface was triggered to sample the signal 5- $\mu$ sec after the switching of each diode. The remaining fixed pattern noise is corrected for by recording dark current and reference spectra at the beginning of each experiment.

The short-term random noise and drift of the spectrometer can be seen in a baseline at 256 nm (Fig. 1). The short-term noise was evaluated by calculating the standard deviation of 50 point sections of the baselines of chromatograms at several wavelengths. Noise levels at the 95% level ( $2\sigma$ ) for the two data acquisition rates used in this work are shown in Fig. 2a. As expected, the increased use of signal averaging at the slower data rate results in a decrease in the noise level by a factor of about 2. Other studies<sup>13</sup> with this spectrometer have shown that up to around 200 averages, the decrease in noise level is proportional to the square root of the number of averages.

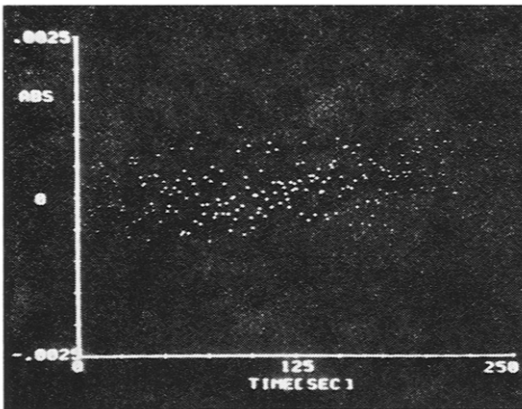


Fig. 1. Baseline at 254 nm. Data rate = 1 spectrum/sec (20 averages). Flow-rate of mobile phase, 0.58 ml/min.

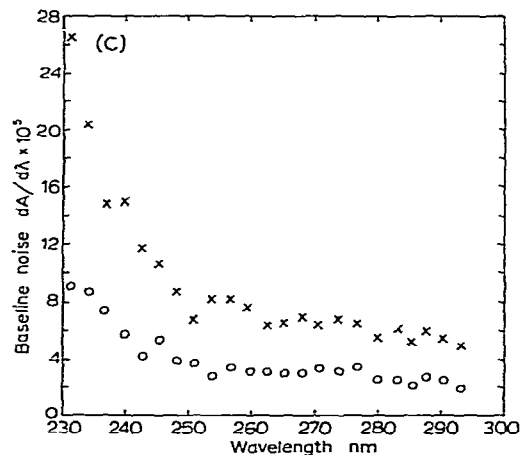
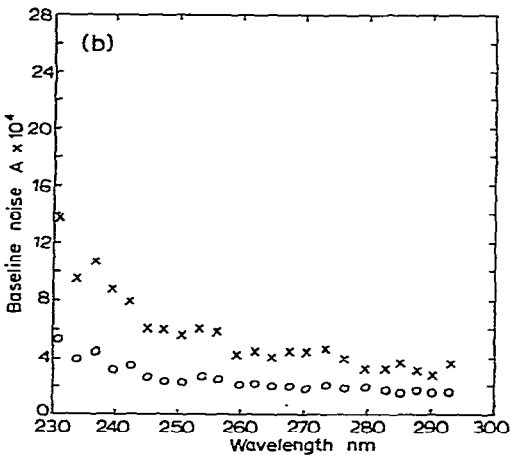
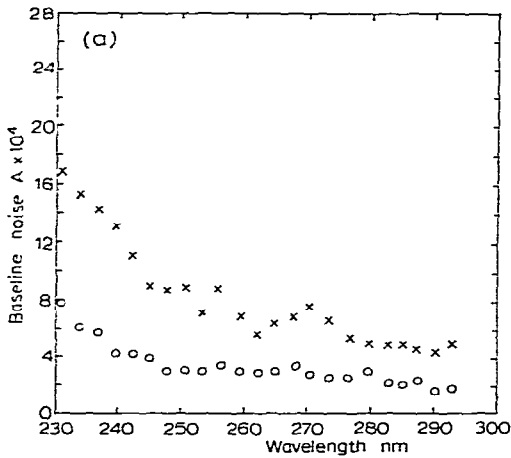


Fig. 2. Baseline noise as a function of wavelength. Averages per spectrum:  $\times$ , 20;  $\circ$ , 94. (a) Unsmoothed; (b) nine-point smooth in wavelength; (c) nine-point derivative in wavelength.

The random noise level can be decreased further by the use of least-squares smoothing<sup>14</sup>. As whole spectra are recorded as a function of time, smoothing can be performed relative to either or both the wavelength and time axes. However, the peaks were too sharp to allow smoothing relative to the time axis without distorting the peak shape. A 9-point quadratic/cubic smooth was used for the wavelength axis, and resulted in a decrease in noise of about a factor of 1.5, as shown in Fig. 2b. For the 1 spectrum/sec data rate (20 averages) the baseline absorbance noise is about  $\pm 0.0012$  a.u. at 231 nm, decreasing to about  $\pm 0.0006$  a.u. at 245 nm and above. The equivalent values for the 1 spectrum per 2 sec rate (94 averages) are  $\pm 0.0005$  a.u. and  $\pm 0.0002$  a.u. Detection limits specified as the peak-to-peak noise levels would be approximately twice these values.

Derivative values can also be calculated by simply changing the coefficients in the smoothing algorithm, and were used for plotting derivative spectra ( $dA/d\lambda$  versus  $\lambda$ ) and chromatograms ( $dA/d\lambda$  versus time)<sup>10</sup>. The baseline noise levels for the derivatives are given in Fig. 2c.

The rapid-scanning spectrometer is a single-beam system, and baseline drift due to long-term source fluctuations can be a significant source of error. The upward slope of the baseline in Fig. 1 corresponds to a drift of about 0.007 a.u./h. This represents a typical level of drift for this system, as the baseline slopes of the chromatograms recorded in this work were generally about  $\pm 0.003$ – $\pm 0.008$  a.u./h. It should be noted that all of the values for random noise and drift given above were obtained under dynamic conditions, with the mobile phase flowing through the column and detector.

Although the plots in Fig. 2 are useful in describing the lower limits of detection for this system, the noise at a finite absorbance will always be greater than baseline noise. The predominant source of noise for the Reticon array is amplifier noise, which is independent of light intensity. The noise as a function of absorbance is given by

$$S_A = S_{A=0} e^{2.3A} \quad (1)$$

where  $S_A$  is the standard deviation (RMS noise) in absorbance and  $S_{A=0}$  is the standard deviation at zero absorbance.

Furthermore, an additional source of random error is present in measuring the peak maxima due to the relatively slow (in comparison with single-wavelength detectors) sampling rate. As the measured retention times may be in error by as much as  $\pm 1/2 \Delta t$ , where  $\Delta t$  is the sampling interval, the measured peak heights will also be in error. Assuming a Gaussian peak shape, the maximum peak sampling error,  $\Delta A$ , is given by

$$\Delta A = A^1 - A^1 \exp - \left[ \frac{(\frac{1}{2} \Delta t)^2}{2\sigma^2} \right] \quad (2)$$

where  $A^1$  is the real peak height and  $\sigma$  is the standard deviation of the peak. For a given  $\sigma$  and  $\Delta t$ , the relative peak height error,  $RE$ , is a constant given by

$$RE = 1 - \exp \left[ - \frac{(\frac{1}{2} \Delta t)^2}{2\sigma^2} \right] \quad (3)$$

Assuming that the variance of the peak sampling error is roughly  $\Delta A^2$ , eqns. 1 and 2 can be combined, and the total relative absorbance or concentration error expressed as

$$\text{Error (\%)} = \frac{(S_{A=0}^2 e^{4.6A} + \Delta A^2)^{\frac{1}{2}}}{A} \cdot 100 \quad (4)$$

Fig. 3 illustrates a typical situation where  $S_{A=0} = 3 \cdot 10^{-4}$  (254 nm),  $\Delta t = 1$  sec and  $\sigma = 3.5 \Delta t$  (the approximate conditions for the elution of benzene in one section of this work). From an absorbance of 0.1–1.5 the error is due primarily to sampling and is constant at 1%. Above and below this range, the error increases sharply due to random noise.

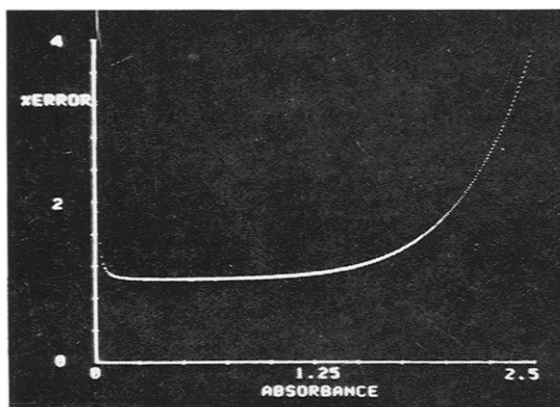


Fig. 3. Relative error calculated from eqn. 4. Conditions used:  $\lambda = 254$  nm;  $S_{A=0} = \pm 3 \cdot 10^{-4}$ ;  $\Delta t = 1$  sec;  $\sigma = 3.5$  sec.

#### Linearity studies

An ideal detector should respond linearly to changes in the concentration of the solute according to the relationship

$$A = KC \quad (5)$$

where  $A$  is the detector signal,  $K$  is a system-dependent constant and  $C$  is the concentration of the solute in the mobile phase. Scott<sup>15</sup> suggested that the following equations should be used for the evaluation of a detector

$$A = KC^r \quad (6)$$

or

$$\ln A = \ln K + r \ln C \quad (7)$$

where  $r$  is the response index of the detector. The response of a detector can be considered to be linear if  $r$  is between 0.98 and 1.02. A plot of  $\ln A$  versus  $\ln C$  allows one to determine  $r$  and evaluate the linearity of the detector in the desired concentration range.

The linearity of the detector was determined with a mixture of three components: naphthalene, pyrene and benzo[*a*]pyrene. Table I shows the results. The second column in the Table gives the wavelength at which the linear range was determined and the third column the number of points used to evaluate *r* via eqn. 7. Table I also shows the linearity when the data are displayed in the derivative mode<sup>9,10</sup>. The wavelength at which the derivative chromatogram is obtained depends on the other solutes. For example, at 252 nm the derivative in the absorbance *versus* wavelength ( $dA/d\lambda$ ) for pyrene and benzo[*a*]pyrene is zero, and thus only naphthalene appears in the chromatogram. Similarly, at 273.8 nm the pyrene peak is the most prominent in the derivative chromatogram. The absorbances of some substances were taken at two wavelengths, *viz.*, the wavelength where the molar absorptivities,  $\epsilon$ , of the solutes are greatest and at wavelengths removed from the maximum  $\epsilon$ .

TABLE I

CHARACTERIZATION OF THE PHOTODIODE ARRAY DETECTOR: DETERMINATION OF THE RESPONSE FACTOR

Compound	Wavelength*	Number of experimental points	<i>r</i>	ln <i>K</i>	Range of amounts injected (mole)		Absorbance or $dA/d\lambda$ range	
					Highest	Lowest	Highest	Lowest
Naphthalene	263 ( <i>A</i> )	13	0.99	16.56	$1.59 \cdot 10^{-7}$	$2.12 \cdot 10^{-10}$	2.55	$3.98 \cdot 10^{-3}$
	252 $\left(\frac{dA}{d\lambda}\right)$	13	1.00	12.96	$1.59 \cdot 10^{-7}$	$2.12 \cdot 10^{-10}$	$6.5 \cdot 10^{-2}$	$9.76 \cdot 10^{-5}$
Pyrene	263 ( <i>A</i> )	13	0.99	17.72	$4.74 \cdot 10^{-8}$	$6.32 \cdot 10^{-11}$	2.60	$4.08 \cdot 10^{-3}$
	235 ( <i>A</i> )	10	0.98	18.34	$1.73 \cdot 10^{-8}$	$6.32 \cdot 10^{-11}$	2.06	$7.78 \cdot 10^{-3}$
	274 $\left(\frac{dA}{d\lambda}\right)$	7	1.00	16.43	$8.63 \cdot 10^{-9}$	$6.32 \cdot 10^{-11}$	0.13	$8.95 \cdot 10^{-4}$
Benzo[ <i>a</i> ]pyrene	285 ( <i>A</i> )	14	1.00	18.48	$5.10 \cdot 10^{-9}$	$1.36 \cdot 10^{-11}$	0.54	$1.49 \cdot 10^{-3}$
	296 ( <i>A</i> )	13	1.01	18.82	$5.10 \cdot 10^{-9}$	$1.36 \cdot 10^{-11}$	0.63	$1.60 \cdot 10^{-3}$
	296 $\left(\frac{dA}{d\lambda}\right)$	12	1.02	16.60	$5.10 \cdot 10^{-9}$	$1.36 \cdot 10^{-11}$	$5.60 \cdot 10^{-2}$	$1.21 \cdot 10^{-4}$

\* *A* indicates absorbance and  $dA/d\lambda$  derivative chromatograms.

Table I seems to indicate that the detector is linear up to about 2.60 a.u. at wavelengths higher than 250 nm and 2.0 a.u. at wavelengths below 250 nm. These upper limits are reasonable as stray light becomes an important factor at such high absorbances and short wavelengths. In the derivative scale the linearity is maintained at 0.13  $dA/d\lambda$  units. The discussion of the noise indicates that the lowest detection limit at wavelengths below 245 nm is about  $1 \cdot 10^{-3}$  a.u., and  $4 \cdot 10^{-4}$  a.u. at higher wavelengths. Therefore, the linear range of the detector seems to be  $2.0 \cdot 10^3$  at 245 nm and  $6.5 \cdot 10^3$  at higher wavelengths.

The data for pyrene clearly show the power of the diode array UV detector. At 235 nm pyrene absorbs very strongly. Fig. 4 shows that the plot of ln *A* *versus* ln *C* for pyrene is not linear at higher concentrations. The data that were fitted to eqn. 7 consisted of only ten experimental points covering the range up to  $1.73 \cdot 10^{-8}$  mole of injected solute. However, if a wavelength of 263 nm was used in the detection of

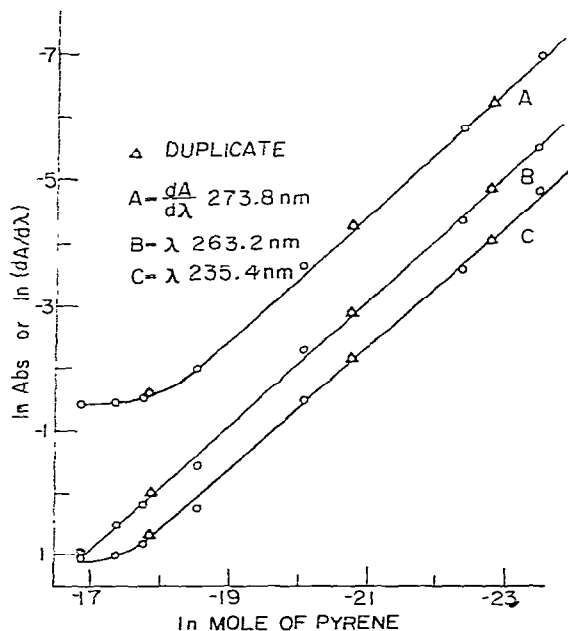


Fig. 4. Determination of the response index from the solute pyrene;  $\Delta$  represents duplicate injections.

pyrene, then the response index was acceptable up to  $4.74 \cdot 10^{-8}$  mole of injected solute. This is shown in the linear plot of  $\ln A$  versus  $\ln C$  in Fig. 4.

Fig. 4 and Table I also shows the results obtained from a plot of  $\ln dA/d\lambda$  versus  $\ln C$  for pyrene at the only useful wavelength, *i.e.*, 274 nm. The deviation from linearity at higher concentrations is clear. The response index was 1.00 only up to  $8.63 \cdot 10^{-9}$  mole of injected solute. The derivative mode of operation seems to be a sensitive indicator of the linearity of the detector.

The discussion above used the weights of injected solutes. The concentrations injected and those seen by the detector are not the same, but are interrelated by the following equation<sup>15</sup>:

$$C_d = \frac{ms}{WQ} \quad (8)$$

where  $C_d$  is the concentration of the solute in the detector when the peak maximum is recorded,  $m$  (g) is the weight of solute injected,  $s$  (cm/min) is the chart speed,  $Q$  (ml/min) is the flow-rate of the mobile phase and  $W$  (cm) is the peak width at 0.607 of the peak height. The data in Table I were converted into  $C_d$ ; however, the trends remain exactly the same as those discussed above.

An alternative means of establishing the linearity of the detector is to plot the detector output against the concentration of the solute injected and to fit the data for the region where the detector is linear, say 0.05–1.5 a.u., to eqn. 5. Using the point where the detector output varies by much more than 5% from the expected response, the linear range can be determined. Fig. 5 shows such plots for pyrene at 235 and 263 nm. The broken line represents a 5% deviation from the expected behavior according



to eqn. 5. The upper limit of detection is taken at the point where the actual absorbance plot crosses the 5% line. From both plots in Fig. 5, it seems that, as might be expected, the detector is linear up to 2.55–2.6 a.u. Fig. 5 again demonstrates the usefulness of the diode array detector; in order to be able to monitor quantitatively large amounts of pyrene the chromatogram should be displayed at wavelengths other than 235 nm. Note that by its very nature, the logarithmic plot in Fig. 4 tends to obscure the deviation from linearity at 263 nm.

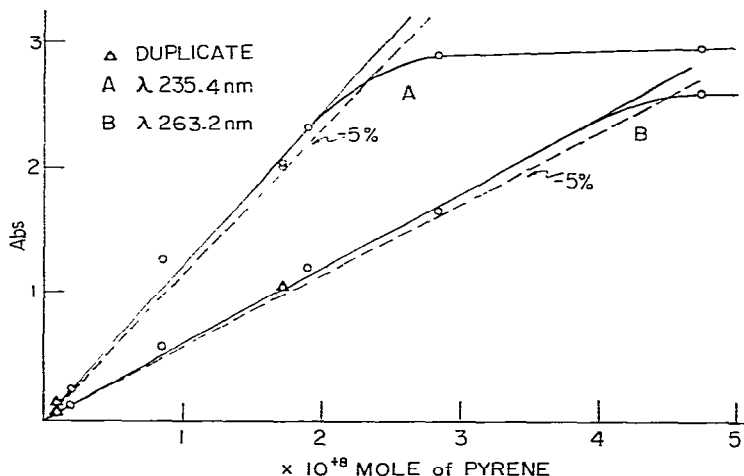


Fig. 5. Absorbance versus amount of pyrene injected at two wavelengths;  $\Delta$  indicates duplicate injections.

The data for naphthalene were treated in the same manner. Although not shown here, plots similar to those in Fig. 5 indicate that the upper detection limit is at about 2.55 a.u. The results agree with the previously stated linear range.

#### *Deconvolution and quantitation of overlapping peaks*

The availability of chromatographic data at more than one wavelength can be utilized to deconvolute unresolved peaks mathematically. Berg *et al.*<sup>16</sup>, Smith and Zetlein<sup>17</sup> and McDowell and Pardue<sup>3</sup> demonstrated that overlapping peaks can be numerically separated. A procedure is described here that employs the entire spectrum to deconvolute the chromatographic peaks of several solutes that overlap severely.

The systems studied included two-, three- and four-component mixtures. Fig. 6 shows a chromatogram of a mixture of benzene, toluene, *p*-xylene and mesitylene plotted at 254 nm. It is clear that the resolution is insufficient for the direct determination of the components. Elution of the pure solutes gave retention times of 274, 280, 285 and 289 sec for mesitylene, *p*-xylene, toluene and benzene, respectively.

A least-squares deconvolution procedure is employed to determine the amount of each component present in the mixtures. The least-squares procedure assumes that the spectrum of the mixtures can be approximated by a linear combination of the spectra of the individual components. Assuming a constant path length, this can be represented as a matrix equation:

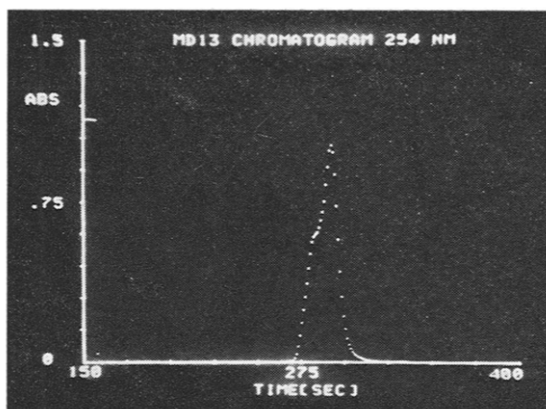


Fig. 6. Chromatogram of mesitylene, *p*-xylene, toluene and benzene displayed at 254 nm. Mobile phase, *n*-heptane at 0.58 ml/min.

$$A = a C \quad (9)$$

where  $A$  is an  $n \times 1$  matrix containing the spectrum of the mixture,  $a$  is an  $n \times m$  matrix containing the spectra of the standards,  $C$  is an  $m \times 1$  matrix containing the concentration of each component relative to the standards,  $n$  is the number of points in the spectrum (128 in this study) and  $m$  is the number of components in the mixture (2, 3 or 4). Although, in the presence of experimental errors in  $A$  and  $a$ , it will not be possible to satisfy eqn. 9 exactly, it is possible to obtain a matrix,  $C$ , that minimizes the sums of the squares of the deviations. It can be shown<sup>18</sup> that the least-squares matrix,  $C$ , is given by

$$C = (a^t a)^{-1} a^t A \quad (10)$$

where  $a^t$  is the transpose of the  $a$  matrix. The residuals plotted in several of the figures are calculated from the following equation

$$R = [(A - a C)^2 / n - m - 1]^{1/2} \quad (11)$$

The standard spectra used in this deconvolution procedure were obtained by taking the spectrum of each pure solute at its chromatographic peak maximum. For mesitylene, *p*-xylene and toluene the results of three runs and for benzene two runs were averaged.

The individual peaks resulting from the least-squares deconvolution of the four-component mixture shown in Fig. 6 are presented in Fig. 7. Although the peaks are well defined, the very small baseline disturbances in the vicinity of the retention time of the other components should be noted. This noise in the baseline can be due to the inherent noise present in the spectra of the standards and of the mixture. Impurities in the standards might also lead to the small negative or positive perturbations.

It is clear from Fig. 7 that the deconvolution technique facilitates the quantitation of the four components. In the present scheme the maxima of the deconvoluted

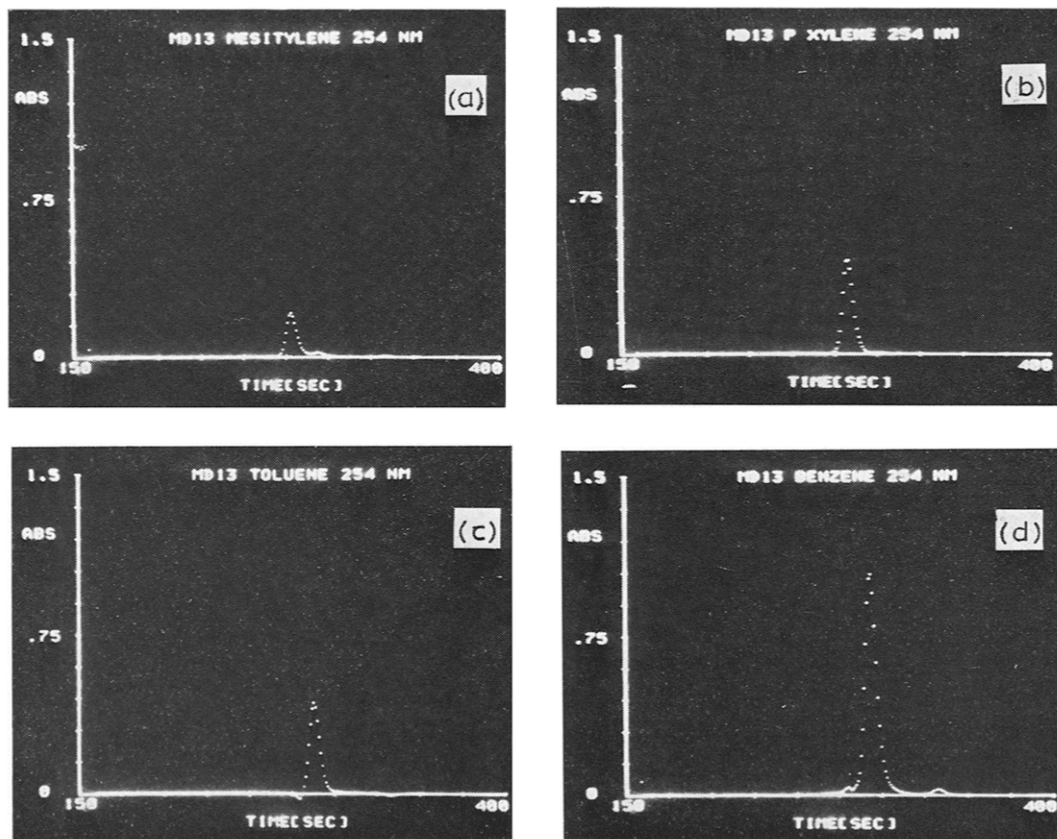


Fig. 7. Results of the least-squares deconvolution of the mixture shown in Fig. 6. (a) Mesitylene; (b) *p*-xylene; (c) toluene; (d) benzene. All chromatograms are displayed at 254 nm.

peaks are multiplied by the known amounts of the standards injected. Table II presents the results obtained from several mixtures of two, three and four components. The maximal error between the amount injected and the amount found is 6.6%, but more typical errors are 3.0% or less. The errors are due to noise in the spectra, injection volume errors and difficulties in the computer determination of the exact position of the maximum of the peak. Some of these errors were recently discussed by Scott and Reese<sup>19</sup> in their work on precision liquid chromatography.

In many analyses, the total number of components in the sample may not be known, and an unknown number of components may overlap in any given chromatographic peak. Over- or under-determination of the samples may thus occur by including excess standards in or excluding necessary standards from the least-squares procedure. Table III presents the results of including excess standards in the least-squares procedure.

Mixture 1 represents the case where all four standards were used to deconvolute a mixture of *p*-xylene, toluene and benzene, and mixtures 2 and 3 show the effects of using three and four standards to characterize a two-component mixture. For the cases studied, very little effect on the accuracy of determination of the components

TABLE II

## COMPARISON BETWEEN THE AMOUNTS OF SOLUTES INJECTED IN A MIXTURE AND THOSE FOUND BY THE LEAST-SQUARES DECONVOLUTION TECHNIQUE

The values for amounts found are averages of triplicate runs.

Mixture No.	Parameter	Mesitylene	<i>p</i> -Xylene	Toluene	Benzene
1	Amount injected ( $\mu\text{g}$ )	—	15.8	15.4	35.1
	Amount found ( $\mu\text{g}$ )	—	16.4	15.0	32.8
	Relative error (%)	—	3.8	2.6	6.6
2	Amount injected ( $\mu\text{g}$ )	—	7.9	15.4	21.1
	Amount found ( $\mu\text{g}$ )	—	8.2	14.9	20.7
	Relative error (%)	—	5.1	3.2	1.9
3	Amount injected ( $\mu\text{g}$ )	—	15.8	15.4	—
	Amount found ( $\mu\text{g}$ )	—	16.2	15.2	—
	Relative error (%)	—	2.5	1.3	—
4	Amount injected ( $\mu\text{g}$ )	13.8	15.8	15.4	35.1
	Amount found ( $\mu\text{g}$ )	14.2	15.8	14.9	33.0
	Relative error (%)	3.6	—	3.2	6.6

TABLE III

## COMPARISON BETWEEN THE AMOUNTS OF SOLUTES INJECTED IN A MIXTURE AND THOSE FOUND BY THE LEAST-SQUARES DECONVOLUTION TECHNIQUE

The number of standards used exceeds the number of components in the mixture; all other conditions as in Table II.

Mixture No.	Parameter	Mesitylene	<i>p</i> -Xylene	Toluene	Benzene
1	Amount injected ( $\mu\text{g}$ )	0	7.9	15.4	21.1
	Amount found ( $\mu\text{g}$ )	0.4	8.4	15.0	20.9
	Relative error (%)	—	6.3	2.6	0.95
2	Amount injected ( $\mu\text{g}$ )	—	15.8	15.4	0
	Amount found ( $\mu\text{g}$ )	—	16.2	14.8	0.7
	Relative error (%)	—	2.5	3.9	—
3	Amount injected ( $\mu\text{g}$ )	0	15.8	15.4	0
	Amount found ( $\mu\text{g}$ )	0.3	16.2	14.7	0.7
	Relative error (%)	—	2.5	4.5	—

in the sample was observed. The finite values found for components not in the sample represent the detection limits of these substances in the presence of the other compounds at the concentration ratios studied.

When the mixture is under-determined, that is to say, the deconvolution method uses less standards than the number of components in the unresolved peak, there are a number of possible results, depending upon the standard eliminated from the least-squares procedure. When the standard omitted has a spectrum that differs from the spectra of the other standards, then results may be obtained that compare favorably with the results from the properly determined analysis. If, however, the standard omitted has a spectrum similar to that of any other standard, the least-

TABLE IV

COMPARISON BETWEEN THE AMOUNTS OF SOLUTES INJECTED IN A MIXTURE AND THOSE FOUND BY THE LEAST-SQUARES DECONVOLUTION TECHNIQUE

The number of standards used is less than number of solutes in the mixture.

Mixture No.	Parameter	Mesitylene	<i>p</i> -Xylene	Toluene	Benzene
1	Amount injected ( $\mu\text{g}$ )	13.8	15.8	15.4	35.1
	Amount found ( $\mu\text{g}$ )	—	17.4	14.9	32.0
	Relative error (%)	—	7	3.2	6.0
2	Amount injected ( $\mu\text{g}$ )	13.8	15.8	15.4	35.1
	Amount found ( $\mu\text{g}$ )	14.3	15.7	28.2	—
	Relative error (%)	4.3	0.6	83.0	—

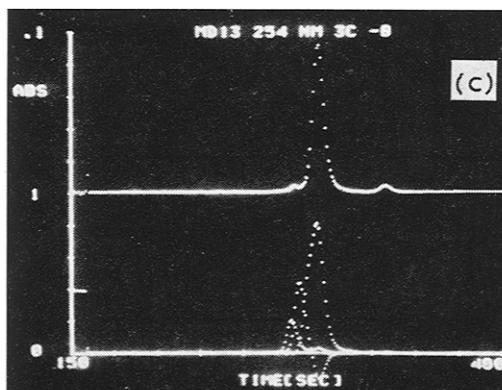
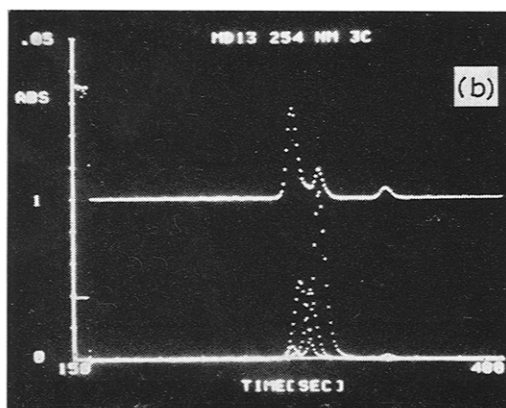
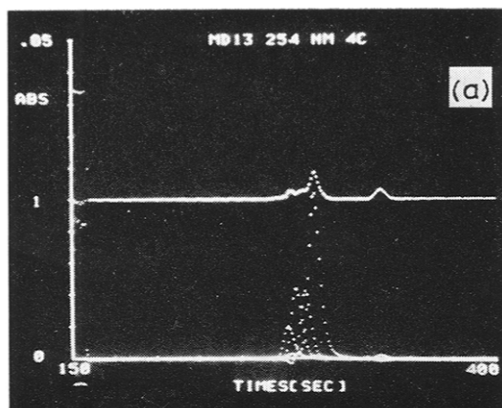


Fig. 8. (a) Resolves of a least-squares deconvolution of a four-component mixture using four standards. Amounts of each solute are given in Table IV. (b) Least-squares results eliminating mesitylene as a standard. (c) Least-squares results eliminating benzene as a standard. The upper half in each figure is the residual using 0.05 or 0.1 a.u.f.s.

squares procedure may yield very erroneous results. Some examples are summarized in Table IV for the four-component mixture. In the first instance, mesitylene was omitted while in the second benzene was not included in the standards set. Fig. 8 shows the deconvoluted chromatograms and the residuals for the four-component mixture. When mesitylene is omitted, the quantitative results are still acceptable and the chromatogram shows no unexpected features. The residuals, however, readily show that some component(s) is (are) missing from the analysis. When benzene is eliminated as a standard, the quantitative result for toluene is very poor. The plot of the deconvoluted chromatogram (Fig. 8c) shows a large negative peak. The residuals also increase greatly over the same time interval as the toluene peak, indicating an extremely poor least-squares fit in this area.

The results presented so far were obtained by using the unsmoothed absorbance spectra of the standards and mixtures in the least-squares deconvolution procedure. The possibility of using the derivative for the absorbance with respect to the wavelength in the least-squares deconvolution procedure was also investigated. The derivatives were generated via a least-squares 9-point quadratic/cubic algorithm<sup>14</sup>. Table V compares the quantitative results obtained using absorbance and derivative procedures. The derivative method required twice the computer time but, as can be seen from Table V, offered no quantitative advantage over the procedure using raw absorbance. This method was therefore not pursued any further.

TABLE V

COMPARISON OF AMOUNTS OF SOLUTES INJECTED IN A MIXTURE AND THOSE FOUND USING ABSORBANCE AND DERIVATIVE LEAST-SQUARES DECONVOLUTION TECHNIQUES

<i>Parameter</i>	<i>p-Xylene</i>	<i>Toluene</i>	<i>Benzene</i>
Amount injected ( $\mu\text{g}$ )	15.8	15.4	35.1
Amount found by absorbance ( $\mu\text{g}$ )	16.8	15.3	33.4
Amount found by derivative technique ( $\mu\text{g}$ )	16.7	15.1	32.3

As discussed previously<sup>3</sup>, it is also possible to deconvolute overlapping chromatographic peaks by plotting  $dA/d\lambda$  versus time at a wavelength where  $dA/d\lambda$  is zero for one of the components. This component is thus effectively eliminated from the chromatogram. If the remaining components in the peak are sufficiently time resolved, the value of  $dA/d\lambda$  at the peaks may be used for quantitation by comparison with standard calibration graphs of  $dA/d\lambda$  versus amount injected. Fig. 9 shows the chromatogram at 254 nm for a mixture of *p*-xylene, toluene and benzene and the plot of  $dA/d\lambda$  versus time at 265.6 nm where  $dA/d\lambda$  for toluene is zero. Table VI presents the quantitative results obtained for *p*-xylene and benzene by applying this method to three different mixtures at the zero crossing wavelength of toluene. Table VI also gives the results obtained for mesitylene in the four-component mixture when  $dA/d\lambda$  versus time is plotted at 266.5 nm, a zero crossing point of *p*-xylene. The accuracy in determining the amount of the solutes using this technique is inferior to that obtained by the least-squares fitting procedure. The derivative method does have one advantage, however. When the zero crossing wavelengths of one of the solutes are known, then one could check whether a chromatographic peak is due to the single

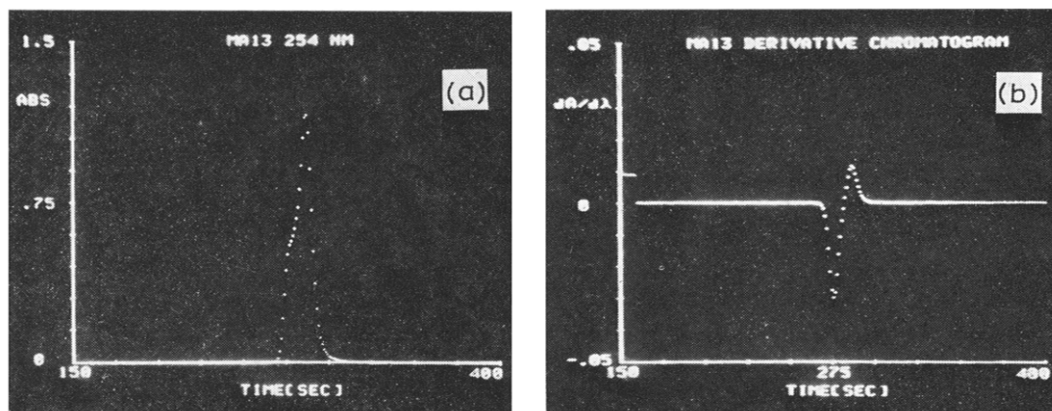


Fig. 9. (a) Chromatogram of a mixture of *p*-xylene, toluene and benzene displayed at 254 nm. Mobile phase, *n*-heptane at 0.58 ml/min. (b) Plot of  $dA/d\lambda$  versus time at 265.6 nm for the same mixture.

TABLE VI

COMPARISON BETWEEN AMOUNTS OF SOLUTES INJECTED IN MIXTURES AND THOSE FOUND USING THE DERIVATIVE ELIMINATION PROCEDURE

Mixture No.	Solute eliminated	Parameter	<i>p</i> -Xylene	Benzene	Mesitylene
1	Toluene	Amount injected ( $\mu\text{g}$ )	15.8	35.1	—
		Amount found ( $\mu\text{g}$ )	16.9	31.0	—
		Relative error (%)	7	11.4	—
2	Toluene	Amount injected ( $\mu\text{g}$ )	7.9	21.1	—
		Amount found ( $\mu\text{g}$ )	8.4	19.0	—
		Relative error (%)	6.3	10.0	—
3	<i>p</i> -Xylene	Amount injected ( $\mu\text{g}$ )	—	—	13.8
		Amount found ( $\mu\text{g}$ )	—	—	13.0
		Relative error (%)	—	—	5.8

solute. A composite peak, when differentiated and re-plotted as  $dA/d\lambda$ , at a zero crossing wavelength, versus time will exhibit a negative or positive peak due to components other than the anticipated solute.

To summarize, the photodiode array detector has been found to be linear over a wide range of absorbances with noise characteristics roughly the same as those of other commercial detectors and the vidicon detector.

There are also some problems with the present system. Firstly, the stability needs to be improved. There are several approaches that can be used to improve stability, including stabilization of the source by optical feedback, monitoring the intensity of the lamp before the sample cell or use of a dual-beam system. Secondly, stray light tends to be relatively high with array detectors, as filters and double monochromators cannot be used. Although the stray light in the present system appeared to be within acceptable limits for the 227–300-nm range covered in this work, it is expected to be more severe when wavelengths below 227 nm are monitored.

Polychromators employing holographically ruled gratings and designed specifically for use with array detectors are now available<sup>20</sup> and should give improved performance. Lastly, the time required to store the data on disc presently limits the data acquisition rate of this system. Higher effective rates (up to 70 spectra/sec) can be achieved by temporarily strong spectra in the core and transferring them to a disc at the end of the component elution or during baseline positions of the chromatogram.

The noise levels at the low-wavelength end of the detector can be reduced by using a different grating, blazed for lower wavelengths than that used in this study. Like the vidicon, the array detector possesses the ability to collect the spectra of the solutes rapidly; however, it is less expensive than the vidicon. The data collected by the diode array detector can be manipulated to deconvolute chromatographic peaks, therefore permitting quantitation of chromatographed solutes when the separation is difficult.

#### ACKNOWLEDGMENT

One of us (E.G.) thanks Whatman for financial support.

#### REFERENCES

- 1 M. S. Denton, T. P. DeAngelis, A. N. Yacynych, W. R. Heineman and T. W. Gilbert, *Anal. Chem.*, 48 (1976) 20.
- 2 A. McDowell and H. L. Pardue, *Anal. Chem.*, 48 (1976) 1815.
- 3 A. McDowell and H. L. Pardue, *Anal. Chem.*, 49 (1977) 1171.
- 4 K. M. Aldous and J. S. Garden, *Pittsburgh Conference on Analytical Chemistry and Applied Spectroscopy, Cleveland, Ohio, March, 1975*, Abstract No. 434.
- 5 R. E. Dessy and W. Nunn, *Pittsburgh Conference on Analytical Chemistry and Applied Spectroscopy, Cleveland, Ohio, March, 1976*, Abstract No. 375.
- 6 R. E. Dessy, W. G. Nunn, C. A. Titus and W. R. Reynolds, *J. Chromatogr. Sci.*, 14 (1976) 195.
- 7 R. E. Dessy, W. D. Reynolds, W. G. Nunn, C. A. Titus and G. F. Moler, *Clin. Chem.*, 22 (1976) 1472.
- 8 R. E. Dessy, W. D. Reynolds, W. G. Nunn, C. A. Titus and G. F. Moler, *J. Chromatogr.*, 126 (1976) 347.
- 9 M. J. Milano, S. Lam and E. Grushka, *J. Chromatogr.*, 125 (1976) 315.
- 10 M. J. Milano and E. Grushka, *J. Chromatogr.*, 133 (1977) 352.
- 11 J. R. Jadamec, W. A. Saner and Y. Talmi, *Anal. Chem.*, 49 (1977) 1316.
- 12 E. H. Snow, *Res. Develop.*, April (1976) 19.
- 13 M. J. Milano and K.-Y. Kim, *Anal. Chem.*, 49 (1977) 555.
- 14 A. Savitzky and M. J. E. Golay, *Anal. Chem.*, 36 (1964) 1627.
- 15 R. P. W. Scott, *Contemporary Liquid Chromatography*, Wiley, New York, 1976.
- 16 R. G. Berg, C. Y. Ko, J. M. Clemans and H. M. McNair, *Anal. Chem.*, 47 (1975) 2480.
- 17 R. N. Smith and M. Zetlein, *J. Chromatogr.*, 130 (1977) 314.
- 18 J. C. Sternberg, H. S. Stills and R. H. Schwendeman, *Anal. Chem.*, 32 (1966) 84.
- 19 R. P. W. Scott and C. E. Reese, *J. Chromatogr.*, 138 (1977) 283.
- 20 J. A. Haas, L. J. Perko and D. E. Osten, *Ind. Res.*, May (1977) 67.